



Macroscopic Alignment of Chromonic Liquid Crystals using Patterned Substrates

Journal:	<i>Physical Chemistry Chemical Physics</i>
Manuscript ID	CP-ART-12-2015-007570.R1
Article Type:	Paper
Date Submitted by the Author:	15-Feb-2016
Complete List of Authors:	Kim, Jeong Yeon; Korea Advanced Institute of Science and Technology, Department of Chemical and Biomolecular Engineering Nayani, Karthik; Georgia Institute of Technology, School of Materials Science and Engineering Jeong, Hyeon Su; Korea Institute of Science and Technology, Institute of Advanced Composite Materials, Soft innovative Materials Research Center Jeon, Hwan-Jin ; National NanoFab Center Yoo, Hae-Wook; Agency for Defence Development Lee, Eun Hyeong; Korea Advanced Institute of Science and Technolgy, Department of Chemical and Biomolecular Engineering Park, Jung; Georgia Institute of Technology, School of Materials Science and Engineering Srinivasarao, Mohan; Georgia Institute of Technology, School of Polymer, Textile and Fiber Engineering, School of Chemistry and Bioche Jung, Hee-Tae; Korea Advanced Institute of Science and Technology, Department of Chemical + Biomolecular Engineering

Title: Macroscopic Alignment of Chromonic Liquid Crystals using Patterned Substrates

Authors: Jeong Yeon Kim^{#1}, Karthik Nayani^{#2}, Hyeon Su Jeong¹, Hwan-Jin Jeon¹, Hae-Wook Yoo¹, Eun Hyung Lee¹, Jung Ok Park², Mohan Srinivasarao^{2,3,4*}, and Hee-Tae Jung^{1*}

Affiliations:

¹National Research Laboratory for Organic Opto-Electronic Materials, Department of Chemical and Biomolecular Engineering, Korea Advanced Institute of Science and Technology, Daejeon, Korea.

²School of Materials Science and Engineering, Georgia Institute of Technology, Atlanta, GA, USA.

³School of Chemistry and Biochemistry, Georgia Institute of Technology, Atlanta, GA, USA.

⁴World Class University Program, Department of Chemical and Biomolecular Engineering, Korea Advanced Institute of Science and Technology, Daejeon, Korea

*Correspondence to: mohan@mse.gatech.edu, heetae@kaist.ac.kr

Co-First authors

Abstract: We demonstrate an efficient technique to align lyotropic chromonic liquid crystals (LCLCs) using secondary sputtering lithography (SSL). Monodomains of LCLCs prepared using SSL maintained their stable alignment for days. A generalization of Berreman's theory was employed to determine the anchoring strength of LCLCs on the tessellated surface patterns. The anchoring energy initially increases with the amplitude (A) of the grooves and excellent alignment of LCLCs was observed when the amplitude of the grooves is equal to half its wavelength (λ). We also note that the anchoring energy levels off above $qA \sim 3$ (where $q = 2\pi/\lambda$), which suggests that increasing qA beyond a certain value does not provide any further advantage for the alignment of LCLCs. This finding provides a useful optimization criterion for the fabrication of the patterned cells to achieve stable monodomain alignment of LCLCs. Our analysis also explains why good alignment of LCLCs has been a difficult task.

Lyotropic chromonic liquid crystals (LCLCs) are fundamentally different from thermotropic liquid crystals in the sense that the aspect ratio of the constituent units is dependent both on temperature and concentration (1-7). The constituent units of LCLCs have flat aromatic cores with water-soluble peripheral groups that enable them to spontaneously assemble into long anisotropic structures in aqueous solutions. LCLCs have the added appeal of being water soluble, hence avoiding the complications of using volatile solvents for processing (8, 9). Further, aligned LCLCs have many interesting properties like dichroism due to their anisotropy of molecular structure. Monodomains of LCLCs on patterned surfaces can preserve their defect free structure when dried from the solution state, opening up many applications like use as polarizing sheets, water based organic electronics and bio sensing applications (8-12).

For using LCLCs in the aforementioned applications, it is essential that there exists a reliable way to obtain defect free monodomains over large areas. In addition, monodomains of LCLCs are essential to carry out fundamental studies for measuring the physical properties of ordered phases such as order parameters, elastic constants, and the anisotropic viscosities (7, 11, 13). Aligning lyotropic systems and polymeric nematics has historically been rather difficult, thus limiting studies aimed at elucidating fundamental properties. Most conventional methods used for aligning small molecule thermotropic materials are not as effective in aligning these systems. There are a few examples, however, in the literature of polymeric systems that have been aligned using non-traditional methods (14-16). Pressure driven extensional flow was used to align solutions of poly(1,4- phenylene-2,6-benzobisthiazole) in methane sulfonic acid. The extruding flow produces alignment of the nematic at the bounding surfaces, which in this case was a rectangular capillary. The alignment can be rationalized with the argument that the velocity of the front at the center of capillary is much greater than at the edges, resulting in the so-called

“fountain flow” where the fluid at the center spills out to the edges of the capillary (16, 17). Solutions of poly- γ -benzyl glutamates have also been aligned to produce monodomains and the elastic constants, various viscosities could be determined (14).

LCLCs bear similarity with polymeric nematics in the sense that the structural units leading to the formation of the nematic phase are long semiflexible rods. Curiously both LCLCs and polymeric nematics are notoriously hard to align using conventional techniques (18, 19). A possible explanation for this is that the anchoring energy (W) provided by conventional rubbing techniques is not sufficiently high for aligning LCLCs and polymeric nematics. Another curious aspect about both polymeric nematics and LCLCs is that the value of the twist elastic constant is significantly lower than the bend and splay elastic constants (7). We believe that the lower energy of twist deformation becomes very relevant in the anchoring energy calculations of LCLCs and polymeric nematics on grooved surfaces because it is possible that the bend and splay deformations relieve some of the energy cost via a twist mode, thus resulting in a lower effective anchoring energy. Hence there is a need for developing techniques that can provide for anchoring energies that are significantly higher than those that are used to align thermotropic materials.

Despite the fact that LCLCs have been studied for over a decade or two, reliable methods for forming stable monodomains are few. Homogeneous alignment of chromonic liquid crystals has been obtained by using an azo-polymer thin film that was irradiated with linearly polarized light (20, 21), by the normal rubbing process as well as evaporating a SiO_x layer (19) has been reported. Superfine abrasive has been used to rub glass substrates and achieve planar anchoring of LCLCs providing weak anchoring (7, 22). Rubbed layer of polyamide has also been used to align LCLCs (23). Very recently alignment of LCLCs has been demonstrated using rubbing and

topographic patterns using nanoimprinting (24, 25). Interestingly when molecular grooves are small enough, LCLCs align perpendicular to the rubbing direction (24). Nanoimprinting is used to generate micro-channels which align LCLCs along the direction of the channels (25). Further, several interesting features in the biphasic regime are reported by the same authors when LCLCs are confined in these tessellated patterns.

Berreman's theory predicts that the anchoring energy increases monotonically as a function of the amplitude (A) of the grooves used to align nematics (26). This was our motivation initially for creating large amplitude patterns using secondary sputtering lithography (SSL). The failure of conventional rubbing techniques to align LCLCs seems to suggest that the amplitude of grooves created by rubbing is not large enough to align LCLCs (27). We have shown in a prior publication that the most common thermotropic liquid crystal, 5CB is well-aligned on surface patterned bifunctional ITO substrates using SSL (28). In this report we use SSL to fabricate nano-sized line patterns of high aspect ratio (ca.15), leading to a tessellated surface that provides sufficiently high anchoring energy for aligning LCLCs. We note that the experimental part is similar to the previously reported work using nanoimprinting (25). The anchoring strength is varied by controlling the height and amplitude of the tessellated patterns (varying qA). An extension of the Berreman theory is used to calculate the anchoring energy. Our study provides a guideline for future experiments on LCLCs for the range of anchoring energies that can provide stable and good alignment. With the analysis presented here we contextualize some of the results present in the literature on aligning LCLCs in terms of the anchoring energy (via qA) and the quality of alignment.

Fabrication of the template began with spin coating a thin polystyrene (PS) film (8 wt% of PS (MW=18,000 g/mol, Sigma Aldrich) solution in anhydrous toluene (Sigma Aldrich)) on an

ITO surface. A pre-patterned poly(dimethylsiloxane) (PDMS) mold with a wavelength (λ) of grooves equal to 500 nm and depth 600 nm was put on the PS coated surface and heated above the glass transition temperature to drive the PS polymer into the spaces of the mold patterns by capillary force. After cooling to room temperature, the mold was removed and PS line arrays were formed on the substrate (Fig. 1a). The PS layer that remained on the bottom of the imprinted structure was subsequently removed by O_2/CF_4 reactive-ion etching (RIE) operated at a flow of 40/60 sccm, a chamber pressure of 20 mTorr, and an RF power of 80 W (Fig. 1b). The target material layer, ITO, exposed at the bottom was etched by Ar^+ ion milling process using the PS layer as a mask, thereby generating line wall structures along the PS pattern shape (Fig. 1c). The PS remaining on top of the target material pattern was completely removed by secondary O_2 RIE operation at a flow of 100 sccm (Fig. 1d). The line amplitude and the wavelength of the pattern can be controlled by employing numerous etching conditions to produce high resolution ITO line patterns over a 5 mm x 5 mm area.

The structural integrity of the patterns was tested using atomic force microscopy (AFM) and scanning electron microscopy (SEM) imaging. Fig. 2a and Fig. 2b show the 2D images of a substrate, observed using the noncontact mode of AFM and SEM. In these representative images, the height of the patterns as measured by AFM was 250 nm and the width of lines is around 20 nm from SEM imaging. Fig. 2c to Fig. 2f show polarized optical microscope (POM) images of the cells filled with Sunset Yellow FCF (SSY) and disodium cromoglycate (DSCG). After sealing the cell with UV curable polymer (Norland Optical Adhesive 63), the cells are heated above the nematic-isotropic transition temperature (T_{NI}) to erase any effects of flow induced alignment.

Results and Discussion:

It is clear from Fig. 2 that the cells show a 90° periodicity under crossed polarizers and have the maximum intensity when the sample makes an angle 45° with the polarizers. This confirms that the alignment caused by the line patterns is efficient in aligning LCLCs. Further to test the efficacy of the method, another LCLC, DSCG, was filled into the patterned structures (Fig. 2e and Fig. 2f). The cell with DSCG is fabricated with substrates having a groove height of 180 nm and the wavelength of the grooves is 500 nm. The behavior of DSCG is similar to SSY in the POM images and shows very good alignment on the surface of the periodic patterns.

To better understand the alignment and to get an estimate of the anchoring strength created by the patterns, we employed Berreman's theory as a first approximation. In his seminal work, Berreman modeled the grooves to be sinusoidal and assumed that the amplitude of the grooves was much smaller than the period (wavelength) of the grooves (26). Berreman also used a single constant approximation to estimate the cost of the elastic deformation. None of these assumptions is strictly valid in our experiments. We note that the Berreman theory gives an accurate estimate of the energy only when the amplitude of the grooves is comparable to the wavelength ($q = 2\pi/\lambda$) of the pattern but overestimates the energy for ($qA > 1$) (29). The approximation of $qA \ll 1$ is clearly invalidated in many experimental conditions (for example, when $A = 300$ nm and $\lambda = 500$ nm). We evaluate the impact of the approximation on the anchoring energy from the numerical calculations reported by Barbero, et al (29).

The surface profile in our studies can be treated as a two dimensional sinusoidal profile in the x-z plane given by

$$z_0 = A(1 + \cos(qx)) \quad (1)$$

In a previous study, it has been shown that the bend and splay elastic constants of LCLCs are quite close to one another, which allows for simplification of the problem with a single constant approximation (7). The total cost of deformation, F , can then be written as:

$$F = \int_0^\lambda \int_0^\infty \frac{K}{2} (\theta_x^2 + \theta_z^2) dx dz \quad (2)$$

where $\theta_x = d\theta/dx$ and $\theta_z = d\theta/dz$ and θ is the angle between the director and the x-axis.

Using the Leibnitz rule, it is straightforward to see that the solution of θ which minimizes the cost of deformation corresponds to the solution of the Laplace equation:

$$\frac{d^2\theta}{dx^2} + \frac{d^2\theta}{dz^2} = 0 \quad (3)$$

with boundary conditions given by:

$$\lim_{z \rightarrow \infty} \theta = 0 \quad \text{and} \quad \theta_0 = \arctan(qA \sin(qx)) \quad (4)$$

When, $qA < 1$, the problem reduces to Berreman's original treatment. However, in our case, that assumption is clearly invalid. Analytical treatment of the problem becomes untenable when $qA \sim 1$, hence one has to resort to numerical methods as was done by Barbero, et al (29). We use their numerical results to estimate the anchoring energies for our experimental system.

As shown in Fig. 3, the values of the anchoring energies calculated from the Berreman's theory are significantly overestimated in the cases where $qA > 1$. A crucial result to note is that

unlike the Berreman analysis, the anchoring energy obtained by the numerical procedure levels off at around $qA=3$. Hence the anchoring energy cannot be increased indefinitely by just increasing the height of the patterns. Also the plot in Fig 3 provides a rather convincing picture of why conventional rubbing techniques do not work well for aligning LCLCs. As can be seen in Fig.3, with the help of the accompanying POM images, we obtain good alignment when $qA \sim 3$. This result leads us to postulate that LCLCs cannot be aligned by conventional rubbing techniques as the amplitude of grooves caused by rubbing is much smaller than those used in our patterns (27, 30). The anchoring energy corresponding to $qA \sim 3$ is 10^{-4} N/m. Anchoring energy around this value appears to be the cut off beyond which one can expect good homogeneous alignment of LCLCs. Comparing this with our previous results of using SSL to align 5CB, we note that the amplitude of the patterns needed to align LCLCs ($A \sim 250$ nm) is much larger than what is needed to align thermotropic liquid crystals ($A \sim 100$ nm) (28). This corresponds to the anchoring energy needed to align LCLCs (10^{-4} N/m) is an order of magnitude larger than that needed to align thermotropic liquid crystals (10^{-5} N/m). Further, using the same analysis we can explain the weak anchoring of LCLCs ($\sim 10^{-6}$ N/m) obtained by using superfine abrasive ($qA \ll 1$) (22, 30). This result again highlights the importance of the use of SSL to achieve the high aspect ratio patterns that are essential to achieve anchoring energies large enough to align LCLCs.

In conclusion, we have successfully demonstrated a way to reliably align LCLCs using SSL. The SSL technique is utilized to make patterns that impose a sufficiently high anchoring strength on the LCLCs to enable good and stable alignment. We conclude that the anchoring strength imposed by this technique (10^{-4} N/m) is higher than what is obtained from conventional rubbing techniques thus enabling the alignment. We observe with the help of POM that anchoring

strength of about 10^{-4} appears to be a cutoff strength below which perfect alignment of LCLCs is not possible. The value of 10^{-4} N/m would serve as a cut off anchoring energy which future experiments seeking to align LCLCs should try to attain to achieve good alignment. Also when the appropriate corrections to the Berreman's theory are taken into consideration, it is noted that the anchoring energy using this technique levels off beyond ($qA=3$), suggesting one cannot achieve higher anchoring strengths just simply by increasing the amplitude of the patterns. Further we postulate that the higher anchoring energy of LCLCs and polymeric nematics is related to their twist elastic constant being about an order of magnitude lower than the bend or splay. Future applications focusing on developing an aligned liquid crystal as a polarizer using SSL which can cover broad visible wavelength by mixing various LCLCs looks very promising. The technique of aligning LCLCs with patterns can also be extended to other fields like bio-sensors.

References:

1. Edwards DJ, *et al.* (2008) Chromonic Liquid Crystal Formation by Edicol Sunset Yellow. *J. Phys. Chem. B* 112(46):14628-14636.
2. Joshi L, Kang SW, Agra-Kooijman DM, & Kumar S (2009) Concentration, temperature, and pH dependence of sunset-yellow aggregates in aqueous solutions: An x-ray investigation. *Phys. Rev. E* 80(4).
3. Kostko AF, *et al.* (2005) Salt effects on the phase behavior, structure, and rheology of chromonic liquid crystals. *J. Phys. Chem. B* 109(41):19126-19133.
4. Lydon J (2010) Chromonic review. *Journal of Materials Chemistry* 20:29.
5. Park HS, Kang SW, Tortora L, Kumar S, & Lavrentovich OD (2011) Condensation of Self-Assembled Lyotropic Chromonic Liquid Crystal Sunset Yellow in Aqueous Solutions Crowded with Polyethylene Glycol and Doped with Salt. *Langmuir* 27(7):4164-4175.
6. Park HS, *et al.* (2008) Self-Assembly of Lyotropic Chromonic Liquid Crystal Sunset Yellow and Effects of Ionic Additives. *J. Phys. Chem. B* 112(51):16307-16319.
7. Zhou S, *et al.* (2012) Elasticity of Lyotropic Chromonic Liquid Crystals Probed by Director Reorientation in a Magnetic Field. *Phys. Rev. Lett.* 109(3).
8. Nazarenko VG, *et al.* (2010) Lyotropic chromonic liquid crystal semiconductors for water-solution processable organic electronics. *Applied Physics Letters* 97(26):263305-263303.
9. Shiyanovskii SV, *et al.* (2005) Real-time microbe detection based on director distortions around growing immune complexes in lyotropic chromonic liquid crystals. *Phys. Rev. E* 71(2).
10. Bae YJ, Yang HJ, Shin SH, Jeong KU, & Lee MH (2011) A novel thin film polarizer from photocurable non-aqueous lyotropic chromonic liquid crystal solutions. *Journal of Materials Chemistry* 21(7):2074-2077.
11. Park MS, Wong YS, Park JO, Venkatraman SS, & Srinivasarao M (2011) A Simple Method for Obtaining the Information of Orientation Distribution Using Polarized Raman Spectroscopy: Orientation Study of Structural Units in Poly(lactic acid). *Macromolecules* 44(7):2120-2131.
12. Lavrentovich M, Sergan T, & Kelly J (2003) Planar and twisted lyotropic chromonic liquid crystal cells as optical compensators for twisted nematic displays. *Liq. Cryst.* 30(7):851-859.
13. Nastishin YA, *et al.* (2005) Optical characterization of the nematic lyotropic chromonic liquid crystals: Light absorption, birefringence, and scalar order parameter. *Phys. Rev. E* 72(4).
14. Taratuta VG, Srajer GM, & Meyer RB (1985) PARALLEL ALIGNMENT OF POLY-GAMMA-BENZYL-GLUTAMATE NEMATIC LIQUID-CRYSTAL AT A SOLID-SURFACE. *Molecular Crystals and Liquid Crystals* 116(3-4):245-252.
15. Toney MF, *et al.* (1995) NEAR-SURFACE ALIGNMENT OF POLYMERS IN RUBBED FILMS. *Nature* 374(6524):709-711.
16. Srinivasarao M & Berry GC (1991) Rheo-optical studies on aligned nematic solutions of a rodlike polymer. *Journal of Rheology* 35(3):379-397.

17. Srinivasarao M (1995) RHEOLOGY AND RHEO-OPTICS OF POLYMER LIQUID CRYSTALS. *International Journal of Modern Physics B* 09(18n19):2515-2572.
18. Tone CM, De Santo MP, & Ciuchi F (2013) Alignment of Chromonic Liquid Crystals: A Difficult Task. *Molecular Crystals and Liquid Crystals* 576(1):2-7.
19. Tone CM, De Santo MP, Buonomenna MG, Golemme G, & Ciuchi F (2012) Dynamical homeotropic and planar alignments of chromonic liquid crystals. *Soft Matter* 8(32):8478-8482.
20. Fujiwara T & Ichimura K (2002) Surface-assisted photoalignment control of lyotropic liquid crystals. Part 2. Photopatterning of aqueous solutions of a water-soluble anti-asthmatic drug as lyotropic liquid crystals. *Journal of Materials Chemistry* 12(12):3387-3391.
21. Ichimura K, Fujiwara T, Momose M, & Matsunaga D (2002) Surface-assisted photoalignment control of lyotropic liquid crystals. Part 1. Characterisation and photoalignment of aqueous solutions of a water-soluble dye as lyotropic liquid crystals. *Journal of Materials Chemistry* 12(12):3380-3386.
22. McGinn CK, Laderman LI, Zimmermann N, Kitzerow H-S, & Collings PJ (2013) Planar anchoring strength and pitch measurements in achiral and chiral chromonic liquid crystals using 90-degree twist cells. *Phys. Rev. E* 88(6):062513.
23. Zhou S, *et al.* (2014) Elasticity, viscosity, and orientational fluctuations of a lyotropic chromonic nematic liquid crystal disodium cromoglycate. *Soft Matter* 10(34):6571-6581.
24. McGuire A, Yi Y, & Clark NA (2014) Orthogonal Orientation of Chromonic Liquid Crystals by Rubbed Polyamide Films. *ChemPhysChem* 15(7):1376-1380.
25. Yi Y & Clark NA (2013) Orientation of chromonic liquid crystals by topographic linear channels: multi-stable alignment and tactoid structure. *Liq. Cryst.* 40(12):1736-1747.
26. Berreman DW (1972) SOLID SURFACE SHAPE AND ALIGNMENT OF AN ADJACENT NEMATIC LIQUID-CRYSTAL. *Phys. Rev. Lett.* 28(26):1683-&.
27. Kumar S, Kim J-H, & Shi Y (2005) What Aligns Liquid Crystals on Solid Substrates? The Role of Surface Roughness Anisotropy. *Phys. Rev. Lett.* 94(7):077803.
28. Jeong HS, *et al.* (2012) Bifunctional ITO layer with a high resolution, surface nano-pattern for alignment and switching of LCs in device applications. *NPG Asia Mater.* 4.
29. Barbero G, Gliozzi AS, Scalerandi M, & Evangelista LR (2008) Generalization of Berreman's model to the case of large amplitude of the grooves. *Phys. Rev. E* 77(5):051703.
30. Davidson ZS, *et al.* (2015) Chiral structures and defects of lyotropic chromonic liquid crystals induced by saddle-splay elasticity. *Phys. Rev. E* 91(5):050501.

Fig. 1.

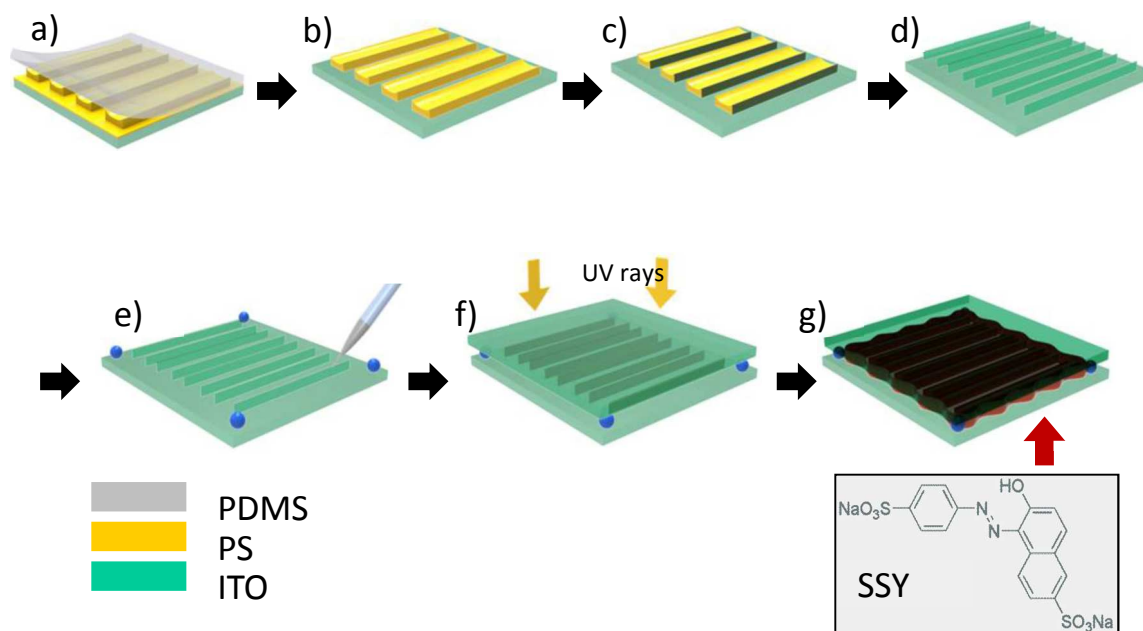


Fig. 1. Scheme of the fabrication of LC cells using secondary sputtering lithography. (a) Line patterns are transferred from PDMS mold to spin-coated PS substrates. (b) Residual PS layer is etched by RIE. (c) Formation of ITO walls by secondary sputtering lithography. (d) Removal of PS template using O_2 plasma, resulting in ITO line pattern. (e) Control of cell gap with PS micro-beads and NOA 63. (f) Upper substrate is placed parallel to bottom substrate. NOA 63 is cured by UV rays. (g) The cell is filled with SSY using capillary force.

Fig 2:

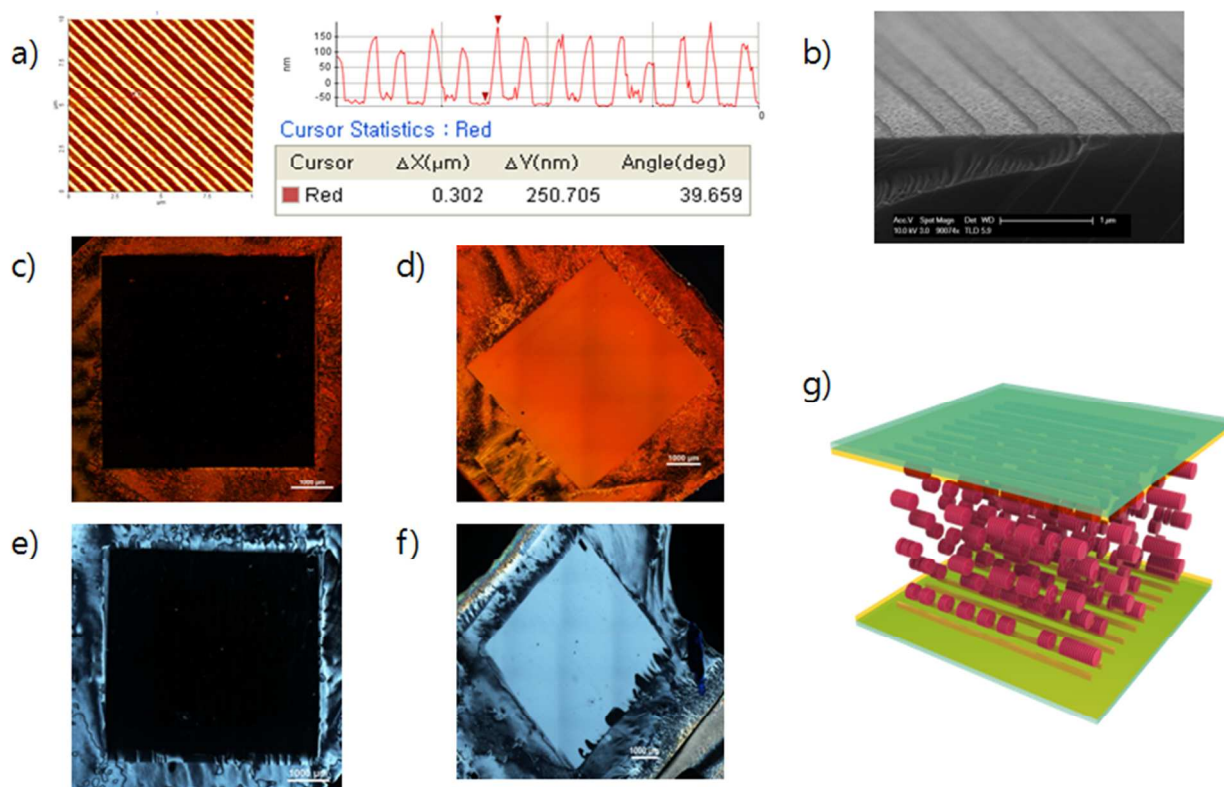


Fig. 2. Alignment of SSY on patterned surfaces. (a) AFM images of the line patterns showing the periodicity and the amplitude of patterns. (b) An SEM image of the patterns. (c) SSY under crossed polarizers with the director parallel to the polarizer. (d) SSY with the director making an angle of 45° with the polarizers. (e) DSCG under crossed polarizers with the director parallel to the polarizer. (f) DSCG with the director making an angle of 45° with the polarizers. (g) Schematic of the alignment of the chormonics along the length of the patterns.

Fig. 3.

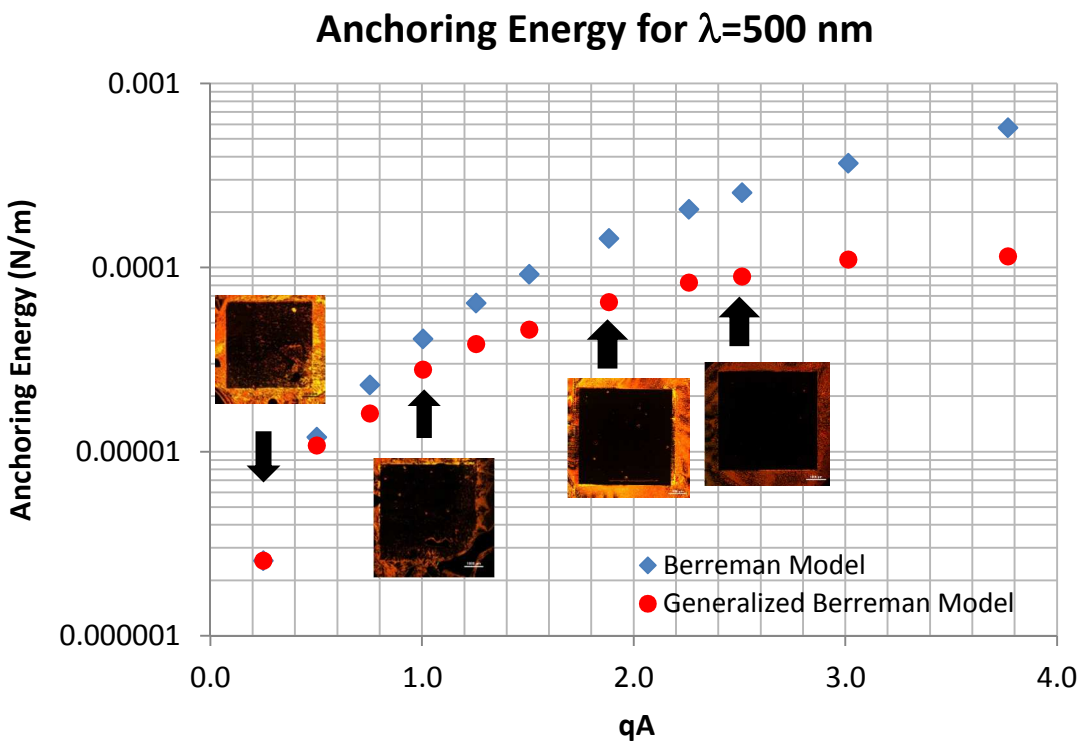


Fig. 3. Calculated values of anchoring energy as a function of qA . Accompanying POM images show the integrity of alignment at different qA . Notice that when $qA < 3$, unaligned regions are present indicating that the alignment is not perfect.

Supplementary Materials:

Materials and Methods:

Sunset Yellow FCF (SSY, 90%, Sigma Aldrich) was purified twice by dissolving in water and reprecipitating using ethanol. Precipitates are vacuum filtrated using micro-porous glass fiber whose pore size is 1 μm . The filtrated powder sample was dried in a vacuum oven over night and kept in a desiccator to remove any trace moisture until used. The purity of the sample was estimated by HPLC to be more than 99 %. All solutions of liquid crystals were prepared with distilled water with a resistivity of 18.2 $\text{M}\Omega\cdot\text{cm}$ (Millipore). The concentration of SSY at room temperature was around 35 wt%. Disodium cromoglycate (DSCG, MP Biomedicals, LLC) at 16 wt% was also used in the experiments.

Commercial ITO glass substrates (20 mm x 20 mm) were purchased from Dasom RMS (Korea) with thickness of 180 nm and transmittance of 96 % at 550 nm. The ITO glass was heated over boiling temperature of isopropyl alcohol (82.5°C) for 10 min, and sonicated in acetone and subsequently in distilled water to remove impurities. The substrates were dried using N_2 blower and then treated by air plasma to functionalize the surface to be hydrophilic.

The LCLCs cells were assembled using two patterned ITO substrates, oriented parallel to each other, with patterned sides in contact with SSY solutions. The cell thickness was controlled by coating a mixture of UV curable adhesive (NOA 63, Norland Product Inc. USA) and PS micro-beads with 10 μm radius at the corners on bottom substrate (Fig. 1e). UV radiation (365 nm) was directed on the cell uniformly to harden the photo curable NOA (Fig. 1f). The LCLCs were loaded by capillary action at room temperature. The cells were immediately sealed with NOA 63 and cured with the UV lamp to prevent solvent evaporation (Fig. 1g). The cell was heated to the isotropic phase on a temperature-controlled stage and cooled down to room

temperature before observation. The state of LC alignment was examined using a polarizing optical microscope (Nikon) under crossed polarizers.

Fig. S1:

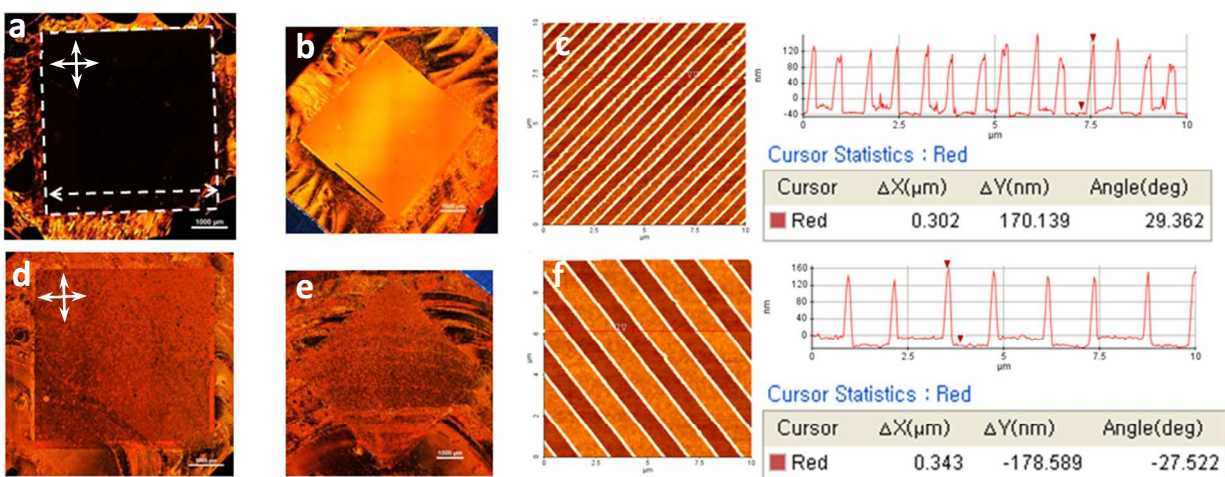


Fig. S1. Alignment of SSY using patterned surfaces. (a,b) POM images of SSY, under crossed polarizers (shown as double arrows), filled in the 5 mm \times 5 mm size of patterned area having 500 nm wavelength and 170 nm amplitude. The dotted arrow in (a) indicates the direction of the grooves, and the sample was rotated 45 $^\circ$ in (b). (c, f) AFM images of the patterned substrates with the feature size of (c) 500 nm wavelength and 170 nm amplitude ($W = 1.8446 \times 10^{-4}$ N/m), and (f) 1000 nm wavelength and 170 nm amplitude ($W = 2.3058 \times 10^{-5}$ N/m). (d,e) POM image of SSY observed as in (a,b), while the patterned area is of 1000 nm wavelength and 170 nm. The scale bars in (a,b,d,e) are 1 mm.